Research Article

COMPARATIVE EVALUATION OF MAXIMUM POWER POINT ALGORITHMS IN PHOTOVOLTAIC SYSTEMS FOR RENEWABLE ENERGY UTILIZATION

Mervenur Kutlu ÇAKIR[1], *Ahmet KAYSAL*[1,*], *Yüksel OĞUZ*[1]

[1]Department of Electrical and Electronics Engineering, Faculty of Technology, Afyon Kocatepe University, Afyonkarahisar, Türkiye

mervemervekutlu8@gmail.com, akaysal@aku.edu.tr, yukseloguz@aku.edu.tr

[*]Corresponding author: Ahmet Kaysal; akaysal@aku.edu.tr

DOI: 10.15598/aeee.v23i1.240902

Article history: Received Sep 3, 2024; Revised Nov 10, 2024; Accepted Dec 30, 2024; Published Mar 31, 2025.

Abstract. *The irregular generation patterns of renewable energy systems lead to undesirable fluctuations in power grids. Integrating energy storage facilities into renewable energy systems is proposed as a solution to this issue. In this study, a photovoltaic energy system with energy storage is designed, and the effects of deterministic and stochastic optimisation-based algorithms on maximum power point tracking are analysed to ensure high-efficiency operation. In the designed system, maximum power point tracking of the photovoltaic system is achieved using the conventional Perturb and Observe, Incremental Conductance, Fuzzy Logic-Based Perturb and Observe, and Particle Swarm Optimization. The algorithms are extensively compared based on performance metrics such as rise time, settling time, and overshoot rate. The Fuzzy Logic-Based Perturb and Observe algorithm exhibits the best performance, with a rise time of 14.28 milliseconds and a settling time of 51.6 milliseconds, achieving the highest efficiency with a battery state of charge level of 69.97%. Detailed simulation analyses conducted in the Matlab/Simulink environment reveal that the fuzzy logic-based method provides faster and more stable results than other methods. Furthermore, a 24-hour real solar irradiance dataset is utilised to test the model under realistic environmental conditions, allowing for a more reliable evaluation of the performance of our storage-integrated photovoltaic.*

Keywords

Fuzzy logic, incremental conductance, maximum power point, particle swarm optimisation, photovoltaic system.

1. Introduction

In recent years, global warming and crude oil prices have led various countries to prioritise investments in renewable energy sources (RES). Solar energy stands out because it applies to small-scale installations and large-scale enterprises. Despite its higher cost than thermal and nuclear energy production, the relatively low energy conversion efficiency of photovoltaic (PV) systems has made optimising maximum power point tracking (MPPT) technologies increasingly critical [1].

Solar energy is generated through panels that meticulously monitor parameters such as solar irradiance and temperature. Power converters are commonly employed to regulate power flow between PV cells and the load [2]. PV cells exhibit a nonlinear I-V curve, continuously employing MPPT algorithms to achieve optimum power under varying environmental conditions [3]. These algorithms adjust the converter's duty cycle based on the PV cells' output to maintain peak power output. The Perturb and Observe (P&O) method, widely recognised in the literature, is noted for its sim-

plicity of implementation but suffers from increased error rates due to oscillations at the maximum point. In recent years, researchers have conducted extensive studies on MPPT in PV energy systems. Methods developed in this field can be broadly classified into two main categories: conventional approaches and soft computing techniques [4]. Among the conventional methods, P&O [5, 6, 7], Global MPPT techniques [8], Incremental Conductance [9], Fractional Open Circuit (FOC) [10], and Fractional Short Circuit (FSC) [11] approaches are widely employed. Frequently used techniques like P&O and IncCond can only track the MPP under uniform irradiance. However, in cases of partial shading, where panels are exposed to varying levels of irradiance, these methods do not perform adequately. Disadvantages of these techniques include low convergence speed, slow tracking performance, and significant oscillations in steady-state conditions. Due to their lower accuracy, FOC and FSC methods are typically preferred for low-power applications. In order to effectively track the MPP under partial shading conditions, conventional methods need to be integrated with other techniques.

In PV research, soft computing and evolutionary algorithms have been proposed as solutions to the limitations of conventional methods. These techniques are considered among the primary choices for nonlinear optimisation because they can handle nonlinear structures, explore extensive search spaces, and reach global optimum regions. Notable techniques used in MPPT applications include Artificial Neural Networks (ANN) [12, 13], Fuzzy Logic Control (FLC) [14, 15], Particle Swarm Optimisation (PSO) [16], and Genetic Algorithms (GA) [17]. Among soft computing techniques, ANN and FLC stand out as knowledge-based systems requiring detailed information for their implementation. While the training process and rule application of these algorithms lead to high memory demands, they are widely preferred for their advantages in responding rapidly and effectively to environmental changes, achieving successful results in nonlinear systems, and minimising steady-state oscillations. In particular, Fuzzy Logic (FL) control can be seamlessly integrated into existing PV systems without requiring prior information on external hardware or system parameters. This integration not only enhances steady-state accuracy but also offers higher tracking speed and reliable performance [15].

The MPP algorithm precisely characterizes the power-voltage (P-V) curve of the PV cell. At the MPP, the power slope is zero, with positive values observed to the left and negative values to the right of this point. This distinctive feature allows the MPP algorithm to optimize the PV cell's output consistently, maximizing energy efficiency [18]. The algorithm operates by determining a reference voltage value for the PV module. This voltage is then communicated to the secondary control loop through a transfer function, ensuring effective regulation [19]. Ullah et al. have presented an MPPT control technique based on FLC to improve MPPT in solar energy generation systems. Supported by simulations conducted in the Matlab/Simulink environment, this method enhances energy efficiency in PV systems by reducing output power fluctuations and increasing system efficiency to 97% [20]. For MPPT in solar energy systems, it offers a highly efficient approach by combining FLC with the Improved Farmland Fertility Optimization algorithm. This new algorithm is specifically designed to improve energy efficiency, particularly under partial shading conditions and environmental variations [21]. Similarly, Kayışlı has developed an MPPT algorithm based on sliding mode control and type-2 FL to enable PV systems to track the MPP more effectively under varying irradiance conditions. The combination of super-twisting sliding mode control and type-2 FL optimizes system efficiency by reducing steady-state fluctuation issues and enhancing stability [22]. Youssef et al. have introduced a reconfigurable FPGA implementation with FLC for MPPT in PV systems. The proposed design offers advantages such as rapid response to varying irradiance and temperature conditions, low cost, and reduced energy consumption. Tests conducted in Matlab/Simulink and VHDL environments highlight the design's flexibility and reconfigurability [23]. Ammar et al. aimed to enhance the fractional-order incremental conductance (FO-IncCond) algorithm for MPPT in PV systems using meta-heuristic optimization techniques. The proposed FO-IncCond algorithm has demonstrated high tracking accuracy and fast response time under variable weather conditions, delivering efficient performance across diverse environmental scenarios [24].

In research conducted by Kabalcı et al., a hybrid microgrid system based on renewable energy sources (RES) has been examined. The designed system consists of 33 kW PV panels, a 100 kW fuel cell, and a 50 kW wind turbine. The IncCond-MPP algorithm has been used for power management, and the wind and fuel cell systems have been controlled with a Proportional-Integral (PI) controller. The system has been tested under various conditions, and its performance has been experimentally verified [25]. A study utilising the IncCond method examined the effects on zeta-converter and buck-boost circuit modelling using a comparative analysis method. Simulations have been conducted under standard test circumstances at 25°C temperature and different irradiance conditions ranging from 100 to 1000 W/m^2. Both DC-DC converters used in the study have been designed for a grid-connected one kWp PV system. The modelling results observed that the efficiencies of both the zeta and buck-boost converters have been maintained at maximum

efficiency with the IncCond algorithm [26]. In another study, optimisation of the IncCond algorithm has been proposed to increase the reliability of MPP tracking in rapidly changing environmental conditions such as temperature and irradiance. This proposed method offers an adaptive approach with variable step size, aiming to enhance the performance of PV systems. The step size, adjusted according to the dynamic system, balances limiting oscillations around the MPP while ensuring rapid and accurate MPP detection [27].

Tab. 1: Comparison of the study with other studies in the literature.

	proposed	**[3]**	**[9]**	**[22]**	**[25]**
P&O	√	x	√	√	x
FL-P&O	√	√	√	√	x
IncCond	√	x	x	√	√
PSO	√	x	x	x	√

In this study, various MPP algorithms are combined to be used in hybrid energy systems, and their effectiveness is evaluated. The block diagram of the simulated RES is given in Fig. 1, and its comparison with other studies in the literature is presented in Tab. 1. Four different MPP methods have been examined in detail: conventional P&O, FL-P&O, IncCond, and PSO. These algorithms have undergone evaluation and analysis across a range of operating conditions. The results significantly contribute to demonstrating that MPP algorithms optimise power generation in hybrid systems most effectively. These analyses facilitate strategic decision-making for more efficient and reliable energy generation in terms of designing and managing energy systems.

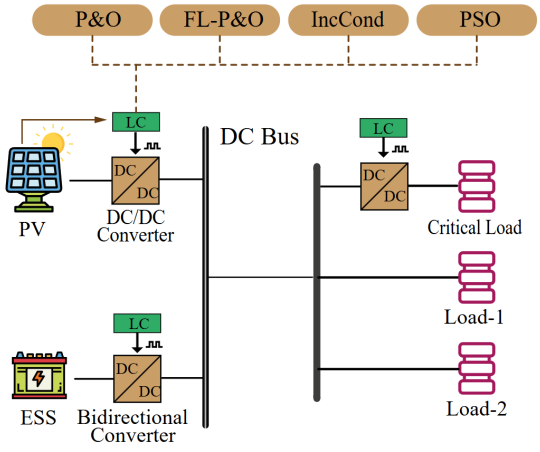

Fig. 1: Block diagram of the simulated renewable energy system.

The main contributions of this paper can be outlined as follows:

1) It presents a comparative analysis of the performance of various MPPT algorithms on a PV energy system with storage. This analysis contributes to identifying suitable algorithms for improving energy efficiency and stability in PV systems by assessing deterministic and stochastic algorithms.

2) By conducting a comprehensive evaluation of deterministic and stochastic optimization-based algorithms in terms of performance metrics such as rise time, settling time, overshoot rate, and battery state of charge, the study clearly highlights the advantages and disadvantages of each algorithm. This detailed performance assessment serves as a guide for the optimal selection of MPPT algorithms in resource-constrained applications.

3) The developed simulation model, elaborated in the Matlab/Simulink environment, provides an opportunity to examine the response of PV energy systems under dynamic conditions. Within this context, the superior performance of the FL-P&O algorithm is emphasized, underscoring its potential for ensuring stable energy production in PV systems.

4) It offers a valuable perspective to the literature on the effectiveness of integrating advanced energy management strategies with storage systems for renewable energy applications. The findings of this study provide important insights and recommendations for the design and improvement of energy management systems.

2. Energy System Components

2.1. Photovoltaic System

PV panels are obtained through numerous PV cells' series and parallel connections. Commonly used in modern solar energy systems, PV cells can fundamentally be described by a single-diode equivalent circuit model. The main components of these cells consist of a diode and a current source. The current produced by PV cells varies in response to changes in solar irradiance levels. In the absence of sunlight, the current source is limited only by the characteristics of the diode. Figure 2 illustrates the commonly used single-diode PV cell model, and Eq. (1)-(2) provides the mathematical expression of this model.

$$I = I_{ph} - I_D \left[\exp\left(\frac{V + IR_s}{aV_{th}}\right) - 1\right] - \left(\frac{V + IR_s}{R_p}\right) \tag{1}$$

$$V_{th} = \frac{kT_c}{q} \tag{2}$$

where I_{ph} represents the current generated in the PV cell, I_D the reverse saturation current, I the output current of the cell, a the ideal diode factor, R_s the cell's series resistance, R_p the cell's parallel resistance, V_{th}

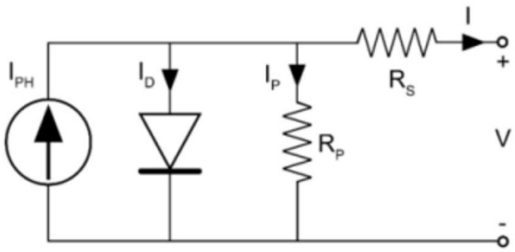

Fig. 2: Single diode equivalent circuit model of a photovoltaic cell.

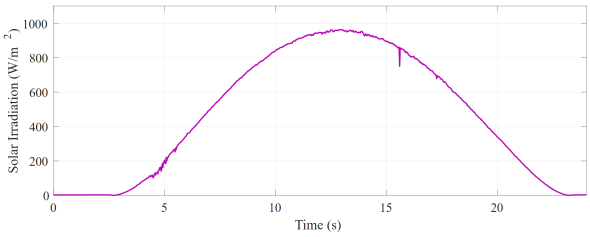

Fig. 3: Real-time daily solar radiation.

the cell's thermal voltage, K the Boltzmann constant, T_c the cell temperature, and q the electron charge [28]. In the designed system, the SunPower SPR-305E-WHT PV module with a power of 305 W has been chosen, and three identical modules have been connected in parallel to a 96 V DC bus via a DC/DC converter. The system's nominal power is 915 W at a temperature of 25°C and solar irradiance of 1000 W/m².

Tab. 2: SunPower SPR-305E-WHT technical data.

Definition	Value
Diode saturation current	$I_0 = 6.3076e^{-12}$ A
Short circuit current	$I_G = 5.95$ A
Current in MPP	$I_{mpp} = 5.57$ A
Open circuit voltage	$V_G = 64.3$ V
Voltage in MPP	$V_{mpp} = 54.8$ V
Number of cells in the module	$N_s = 96$
Shunt resistance	$R_{sh} = 393.2054\Omega$
Series resistance	$R_s = 0.37428\Omega$

In the RES model developed in the Matlab/Simulink environment, actual solar irradiance data obtained from the coordinates 38°49'02.7"N and 30°31'56.7"E on October 12, 2024, have been used in addition to constant irradiance scenarios. The dataset shown in Fig. 3 covers an irradiance range of 0 to 960 W/m², enabling the PV system to perform under realistic environmental conditions. This approach goes beyond analyzing the system's behaviour under steady-state conditions, providing a model that closely approximates the variable conditions encountered in real-world scenarios.

2.2. Energy Storage System

Lithium-based batteries offer distinctive features such as high energy density and long lifespan. These characteristics enable their use across various applications, from portable devices to electric vehicles. Lithium batteries' high energy storage capacities result in longer usage life and more effective energy storage, meeting industrial and consumer demands. Today, lithium-based batteries are favoured as the most economical solution for meeting the energy needs of electrical systems. Key factors influencing the selection are their energy and power density, almost complete coulomb efficiency, extensive cycle life, lack of memory effect, and minimal self-discharge rate [29].

Tab. 3: Lithium-ion battery technical data.

Definition	Value
Nominal voltage	$V_b = 48$ V
Nominal capacity	$Q_{nom} = 5$ Ah
Nominal discharge current	$I_{dis} = 2.1739$ A
Initial charge level	$SOC = 70\%$
Battery internal resistance	$R_b = 0.096\ \Omega$

According to the lithium-ion battery data provided in Tab. 3, the battery's nominal voltage is 48 V, and its capacity is 5 Ah. The battery output voltage is expressed by Eq. (3), while Eq. (4) describes the variation in the battery's state of charge depending on the battery current and capacity.

$$V_b = V_0 - R_s I_b - K\frac{Q}{Q - \int_0^1 I_b dt} + Aexp\left(-B\int_0^1 I_b dt\right) \tag{3}$$

$$SOC = SOC_{ini} - \int_0^1 \frac{\eta I_b}{Q} dt \tag{4}$$

where V_b represents the battery terminal voltage, V_0 and I_b the battery's open circuit voltage and nominal current, respectively, R_s the internal resistance, A and B the battery's exponential voltage and capacity, K the polarisation constant, SOC_{ini} the initial state of charge, and Q the battery capacity, η the battery efficiency [30]. In PV systems, batteries provide a backup energy function during insufficient sunlight or at night when energy demand persists. With these capabilities, lithium batteries play a critical role in enhancing the reliability and efficiency of solar-powered systems.

3. Algorithms Used in Photovoltaic Systems

3.1. Perturb and Observe Algorithm

The P&O method is a commonly utilised algorithm within the field. This technique continuously monitors the power fluctuations of the PV module, subsequently controlling the direction of voltage changes in the module. Based on this information, adjustments to the duty cycle are made for future updates and corrections. Typically, the power and voltage characteristics of the module are employed to track the operational point of the module output [31]. The flowchart for the P&O algorithm is presented in Fig. 4. Upon examining the flowchart of the P&O algorithm, the initial step involves measuring the system's power output. Next, the voltage of the PV module is slightly increased or decreased. After this adjustment, the new power value is compared with the previous one. If the power value has increased, the change is in the correct direction, and the adjustment in the same direction continues. If the power has decreased, the voltage change is made in the opposite direction. This process is repeated until the system reaches the MPP. The algorithm iteratively adjusts the voltage until it finds the value closest to the optimal power point.

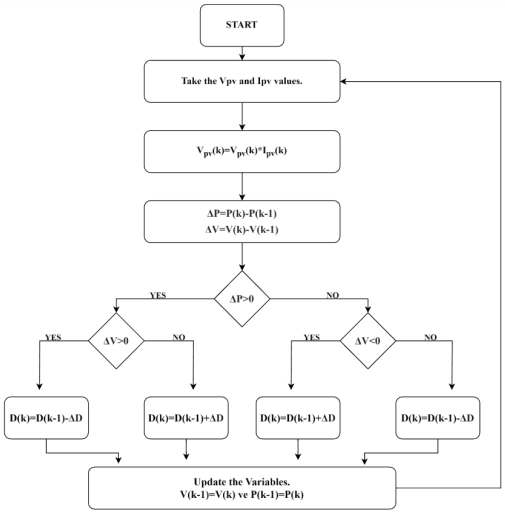

Fig. 4: Perturb and Observe algorithm flowchart.

3.2. Fuzzy Logic Based Perturb and Observe Algorithm

FL is an artificial intelligence approach used to solve problems containing uncertainties. Unlike conventional methods, this method evaluates input data under fuzzy concepts within certain rules. FL algorithms systematically make inferences using these fuzzy concepts and obtain results. This method has advantages such as the ability to handle uncertainties, the capability to model complex systems, and the flexibility to cope with real-world data.

Figure 5 illustrates the Mamdani-type fuzzy inference system, which comprises four main components: input-output membership functions, a set of fuzzy rules, a fuzzy inference engine, and a defuzzifier. The FL controller is structured around two inputs and one output. The input variables are error and the rate of change of the error, while the output variable is a pulse width modulation signal used to drive the switching element. Both inputs are fuzzified using FL. This logic encompasses seven fuzzy subsets: positive big (PPB), negative big (NNB), negative medium (NM), positive medium (PM), negative small (NNS), positive small (PPS), and zero (Z) [3].

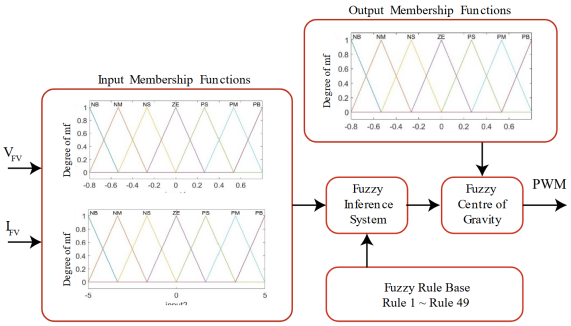

Fig. 5: Fuzzy inference system block diagram.

Various membership functions such as Gaussian, trapezoidal, triangular, bell curve, and sigmoid are available in FL. In this study, triangular membership functions shown in Fig. 5 have been preferred. This type of function relies on three main parameters: the start (α), the end (c), and the highest degree of membership (b), and is defined in Eq. (5). Finally, the fuzzy output is converted into a crisp control signal in the defuzzification process. This process uses the centre of gravity method defined in Eq. (6).

$$\mu(x;a,b,c) = \begin{cases} a < x < b \rightarrow \frac{(x-a)}{(b-a)} \\ b < x < c \rightarrow \frac{(c-x)}{(c-b)} \\ x < a \text{ or } x > c \rightarrow 0 \end{cases} \tag{5}$$

$$x^*_{COG} = \frac{\sum_{i=1}^{n} x_i \mu(x_i)}{\sum_{i=1}^{n} \mu(x_i)} \tag{6}$$

where x_i is the output of the i_{th} fuzzy rule, $\mu(x_i)$ is the inference result of the i_{th} fuzzy rule, and x^*_{COG} is the output of the fuzzy controller. In FL, the rule table used to determine input and output values is shown in Tab. 4. An FL rule table is used to determine the outputs corresponding to a specific input combination. This table defines the behavior of the FL, specifying which outputs should occur under which conditions.

Tab. 4: Fuzzy inference system rule table.

e/de	NNb	NM	NNS	Z	PPS	PM	PPB
NNB	Z	Z	Z	NNB	NNB	NNB	NNB
NM	Z	Z	Z	NM	NM	NM	NM
NNS	NNS	Z	Z	NNS	NNS	NNS	NNS
Z	NM	NNS	Z	Z	PPS	PM	PPB
PPS	PM	PPS	PPS	PPS	Z	Z	PPS
PM	PM	PM	PM	PM	Z	Z	Z
PPB	PPB	PPB	PPB	PPB	Z	Z	Z

3.3. Incremental Conductance Algorithm

The IncCond algorithm is a widely used approach in adaptive control applications. This algorithm represents an iterative process to optimise system behaviour. The initial step determines the system's starting condition. Subsequently, objectives are defined. An initial estimate representing the current state of the system is made. Based on this estimate, the control signal is calculated, and the system's state is updated. The system's behaviour is then reviewed to assess whether the objectives have been met. The control calculation and application are repeated if the objectives have not been reached or the specified criteria have not been met. These steps are repeated until a specific termination condition is met [32].

The IncCond algorithm identifies the peak of the P-V curve by analysing its slope, aiming to locate the MPP. In this approach, the incremental conductance (dI/dV) and instantaneous conductance (I/V) are calculated to track the MPP. The relationship between these two values determines the position on the PV module's P-V curve, utilising Eq. (7) to (9). Equation (7) indicates that the PV module is operating at the MPP, while Eq. (8) and (9) signify that the module is operating to the left and right of the MPP on the P-V curve, respectively.

$$\frac{di}{dv} = -\frac{I}{V} \tag{7}$$

$$\frac{di}{dv} > -\frac{I}{V} \tag{8}$$

$$\frac{di}{dv} < -\frac{I}{V} \tag{9}$$

$$I + V\frac{di}{dv} = 0 \tag{10}$$

The IncCond algorithm uses Eq. (10) to detect the MPP. The MPP tracking system's control device measures the PV module's voltage and current. If Eq. (8) and (9) are satisfied, the converter's duty cycle should be decreased or increased, respectively. If Eq. (10) is satisfied, no change should be made to the duty cycle [33].

3.4. Particle Swarm Optimisation

PSO is a recognised technique among control algorithms for tracking the MPP in PV systems. This algorithm has been developed to maximise power output under variable weather conditions. Inspired by the social behaviours of birds or fish, the traditional PSO method aims to find the optimal solution by utilising a swarm of particles moving in a multidimensional search space. This method has proven effective in tracking the MPP in PV system controls, managing to deal efficiently with low-frequency oscillations. In order to track the MPP, the positions and velocities of the particles are optimised by continuously updating the duty cycle of the DC/DC converter [34]. Initially, this method starts with a randomly distributed particle population where each particle represents a potential solution. The positions and velocities of the particles are altered using updated equations that consider both individual and collective experience histories [35].

When used for MPP tracking in PV panels, each particle calculates parameters typically representing output variables such as voltage or current. As these particles progress through the problem space, they evolve towards the best solution, thereby maximising power output from the PV panel. In this way, PSO is an effective method for enhancing the efficiency of solar energy systems.

4. Results and Discussion

This study involves a comparison of MPP control techniques used in the power production of PV systems. Modelling and simulation studies have been conducted in the Matlab/Simulink environment, addressing four operating conditions. The voltage stability of the storage-integrated PV system, created using PV panels, has been examined according to critical and variable load profile scenarios. The proposed storage-integrated PV system utilised the PV panel parameters listed in Tab. 2 and the lithium-based battery parameters specified in Tab. 3. The time-dependent changes in scenarios related to the storage-integrated PV system are illustrated in Fig. 6.

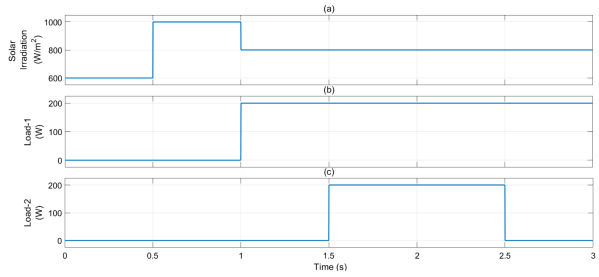

Fig. 6: Time-dependent changes in scenarios for the storage-integrated PV system.

In the simulation study, the initial charge level of the energy storage unit has been set at 70%. The simulation model analysed commonly preferred methods such as conventional P&O, FL-P&O, IncCond, and PSO. The system performance has been evaluated in detail using these four different methods. The simulation ran for a duration of 3 s. The solar irradiation level applied to the PV panel started at 600 W/m², was increased to 1000 W/m² at 0.5 s, and then reduced back to 800 W/m² at 1 s. This irradiation level and duration have been maintained for all algorithms. In addition to a critical load of 600 W, two loads, each with a capacity of 200 W, referred to as Load-1 and Load-2, have been included in the system. The time-dependent changes in the loads are depicted in Fig. 6 (b) and (c). The effects of different algorithms on PV and battery power, the optimisation of energy transfer, and their responses to system dynamics are detailed in Fig. 7. The time-dependent changes in PV power and lithium-based battery power can be observed in Fig. 7 (a) and (b), respectively.

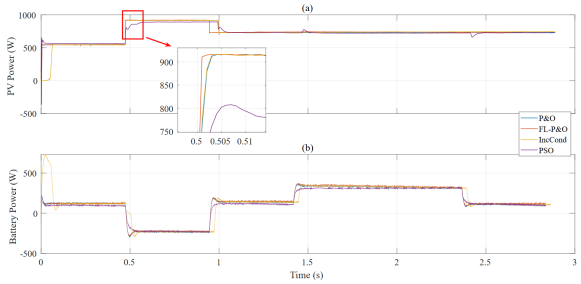

Fig. 7: Change of power in photovoltaic and energy storage unit.

Upon examining Fig. 7 (a), it is observed that right from the start of the simulation, the FL-P&O algorithm, informed by expert opinion, met a 543 W energy demand in just 1 ms, displaying a significant speed advantage over other algorithms. Moreover, the conventional P&O algorithm reached the MPP of the PV power in 6 ms, while the system operated by the IncCond algorithm completed this in 75 ms. Similarly, the PSO algorithm exhibited a variable power profile characterised by sharp declines and rises, achieving system stability within 20 ms. During the initial 0.5 s, while only a critical load of 600 W was active in the system, the entire 543 W power demand was met by the PV system, and the battery group supplied the remaining power demand.

At 0.5 s, solar irradiation has been increased from 600 W/m² to 1000 W/m². The installed capacity of the PV system, 915 W, has been fully transferred by all MPP algorithms except for the PSO algorithm, which has been limited to 891 W. During this period, while the critical load has been entirely powered by the PV system, 315 W of energy has been stored in the battery group. At 1 s, the solar irradiation value dropped to 800 W/m² and remained at this level until the end of the simulation. As seen in Fig. 6, Load-1 has been activated at 1 s and Load-2 at 1.5 s. Load-1 and Load-2, including the critical load, have been steadily supplied throughout the simulation.

In the storage-integrated PV system, a performance comparison of the bus voltages has been provided in Fig. 8. When evaluating the performance of the algorithms, the characteristics related to each one's initial response, stability, and peak performance have been examined. The storage-integrated PV system has been connected to a common DC bus with a nominal voltage of 96 V. Upon the start of the simulation, the bus voltages for FL-P&O, conventional P&O, PSO, and IncCond algorithms have respectively dropped to 95.13 V, 94.39 V, 92.76 V, and 90.47 V, and have then quickly risen back to the reference bus voltage, maintaining their voltage stability. During load changes in the system, it is visible from Fig. 8 that the FL-P&O algorithm has restored the reference voltage more quickly than others.

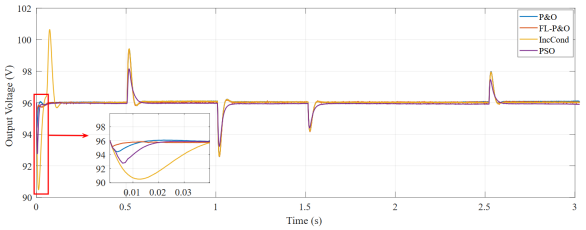

Fig. 8: Comparative graphs of PV panel output voltage for maximum power point algorithms.

Throughout the simulation, the changes in the DC bus voltage obtained using different algorithms have been calculated as the highest positive ε_k^+ and lowest negative ε_k^- voltage regulation values according to Eq. (11) and (12) [36].

$$\epsilon_k^+ = \frac{\overline{u_k} - \min(u_k)}{\overline{u_k}} \cdot 100 \tag{11}$$

$$\varepsilon_k^- = \frac{\overline{u_k} - \max(u_k)}{\overline{u_k}} \cdot 100 \tag{12}$$

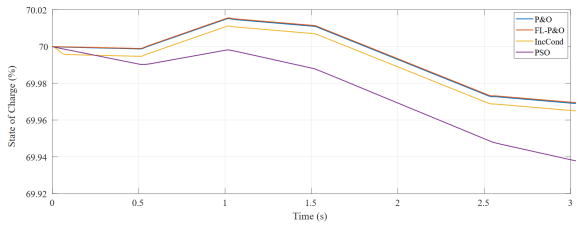

Fig. 9: Change in SOC levels under variable load conditions.

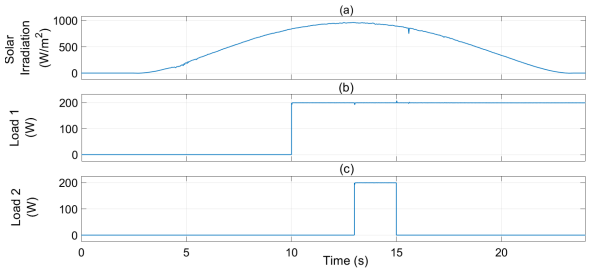

Fig. 10: Time-dependent variation of actual solar data, Load1 and Load2.

where, $\overline{u_k}$ represents the reference bus voltage and u_k denotes the voltage value at the time of operation. After the system stabilised, the highest positive fluctuation in the bus voltage occurred at 0.5 s, and the largest negative fluctuation occurred at 1 s. Upon examining the 80 ms oscillations, the highest fluctuations have been observed with the IncCond algorithm, where ϵ_k^+ and ε_k^- have been calculated as +3.44% and -3.54%, respectively. These values are within the limits set by the IEEE 1547-2003 standard.

The responses of MPP tracking algorithms to a unit step input have been compared based on overshoot, rise time, and settling time performance metrics. They are detailed in Tab. 5. While the PSO algorithm has the best overshoot value at 9.57%, the FL-P&O algorithm stands out in terms of performance with a rise time of 14.281 ms and a settling time of 51.606 ms. According to the findings, when comparing overshoot values, the PSO algorithm performs 56.03% better than its closest competitor, the FL-P&O algorithm. Regarding rise time, FL-P&O performs similarly to the nearest conventional P&O algorithm by a margin of 3.708%. These results demonstrate that FL-P&O is superior to the conventional P&O algorithm.

In the simulation studies conducted in the PV system, changes in battery State of Charge (SOC) levels are presented in Fig. 9. Beginning with a SOC of 70%, the energy requirements of the load are supplied by both the PV panel and the battery, resulting in a reduction of the SOC level. At 0.5 s, as solar irradiance increased from 600 W/m^2 to 1000 W/m^2, not only was the critical load continuously powered, but the battery group also began to charge. However, at 1 s, with the activation of Load-1 and the decrease in solar irradiance to 800 W/m^2, the PV system could not meet the total demand alone, and the battery switched to discharge mode. At the end of the simulation, the FL-P&O algorithm provided the best result, with a SOC level of 69.97%.

The 24-hour solar irradiance data presented in Figure 10 were measured using a pyranometer and covered an irradiance range from 0 to 960 W/m^2. These actual solar radiation data enable a more detailed examination of PV system performance under realistic environmental conditions. The daily irradiance data were scaled to 24 s and utilized in the simulation studies accordingly.

In the simulation studies, the initial charge level of the energy storage unit was set at 70%. As in other studies, performance analyses of four different MPPT algorithms were conducted within this simulation model, focusing on PV power and battery power, and the results are presented in Fig. 11. The findings indicate that, compared to other algorithms, the PSO algorithm was unable to fully track the maximum power and was affected by load variations.

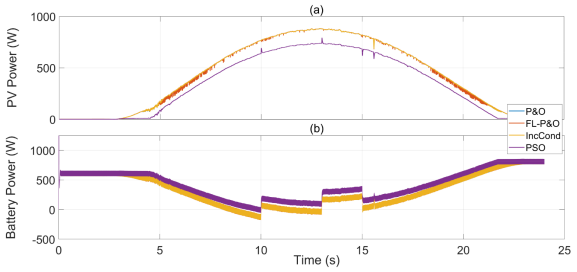

Fig. 11: Change of power in photovoltaic and energy storage unit.

This study presents a comparative analysis of various MPPT algorithms within a PV energy system equipped with energy storage, focusing on performance metrics such as rise time, settling time, and battery state of charge. Based on the findings of the study, the following recommendations are presented:

1) The FL-P&O algorithm demonstrates superior performance in terms of response time and stability. It is recommended that this method be preferred in PV systems where high precision and stability are critical, especially in applications requiring rapid adaptation to irradiance changes.

2) The integration of lithium-based energy storage systems into PV systems has been found effective for maintaining stable voltage and providing backup energy during fluctuations in energy production. Incorporating energy storage units into PV systems operating under variable irradiance conditions is recom-

Tab. 5: Performance comparison of MPP tracking algorithms.

Parameters	P&O	FL-P&O	IncCond	PSO
Overshoot (%)	17.40	17.08	21.56	9.57
Rise time (ms)	14.831	**14.281**	30.954	15.407
Settling time (ms)	52.057	**51.606**	97.605	68.668

mended to enhance energy supply security and availability.

3) Although this study is conducted in a simulation environment, testing these algorithms under real-world conditions will be essential for evaluating their practical effectiveness. Experimental studies across different PV configurations and varying environmental conditions would provide valuable insights into the resilience of each MPPT algorithm.

5. Conclusion

This study aims to identify the most effective solution for PV systems by analysing the performance of MPP tracking algorithms that employ various strategies, including artificial intelligence and meta-heuristic optimisation. When compared with other algorithms, such as conventional P&O, IncCond, and PSO, the FL-P&O method has demonstrated a distinct superiority in enhancing the energy efficiency of PV systems. In simulations conducted under similar conditions, the FL-P&O method successfully met a 543 W energy demand within just 1 ms. In contrast, the conventional P&O method reached the MPP in 6 ms, while the PSO algorithm achieved system stability in 20 ms, and the IncCond algorithm took 75 ms to stabilise the system. This speed difference illustrates how effective the FL-P&O method is in adapting PV systems to dynamic environmental changes.

The responses of MPP tracking algorithms to a unit step input have been analysed based on overshoot, rise time, and settling time performance metrics. According to the results, the PSO algorithm possesses the best overshoot value at 9.57% in voltage amplitude. In contrast, the FL-P&O algorithm stands out with a rise time of 14.28 ms and a settling time of 51.6 ms. The FL-P&O method provides faster response times and better system stability than other methods and demonstrates superior performance in the rise and settling times. During the increase in solar irradiance from 600 W/m^2 to 1000 W/m^2, the FL-P&O method successfully transmitted the system's maximum installed power of 915 W, whereas the PSO method was limited to 891 W under the same conditions. This case indicates that the FL-P&O method more effectively tracks the MPP and responds quickly to sudden increases in solar irradiance. Similarly, when examining the changes in battery SOC levels, the FL-P&O algorithm has given the best result, with 69.97%.

The findings demonstrate that the FL-P&O approach can enhance the energy efficiency of PV systems due to its ability to respond quickly and effectively to environmental variables. Furthermore, it reveals that FL effectively detects the MPP and maintains system stability. Lastly, according to the results of this study, the FL-P&O method has the potential to contribute to the sustainability of global energy systems and play a significant role in energy transformation processes. Future studies could focus on optimizing these algorithms under various environmental conditions and in real-time applications. Testing their applicability with different PV system configurations or other renewable energy sources is also recommended. Experimental validation in field conditions, complementing this simulation-based study, would be valuable for revealing the real-world performance of the algorithms.

Author Contributions

M.K. and A.K. were responsible for conceptualising and designing the study. M.K. procured materials, and A.K. handled data collection and processing. A.K. and Y.O. conducted the analysis and interpretation of the data. M.K. conducted the literature search, and both M.K. and A.K. contributed to writing the manuscript. The manuscript underwent critical review by A.K. and Y.O.

References

[1] CHENG, P.-C., B.-R. PENG, Y.-H. LIU, J.-W. HUANG. Optimization of a fuzzy-logic-control-based MPPT algorithm using the particle swarm optimization technique. *Energies*. 2015, vol. 8, iss. 6, pp. 5338–5360. DOI: 10.3390/en8065338.

[2] SHIAU, J.-K., Y.-C. WEI, B.-C. CHEN. A study on the fuzzy-logic-based solar power MPPT algorithms using different fuzzy input variables. *Algorithms*. 2015, vol. 8, iss. 2, pp. 100-127. DOI: 10.3390/a8020100.

[3] EYDI, M., S. I. HOSSEINI SABZEVARI, R. GHAZI. A novel strategy of maximum power point tracking for photovoltaic panels based on fuzzy logic algorithm. *Advances in Electrical and Electronic Engineering*. 2020, vol. 18, iss. 1, pp. 1-10. DOI: 10.15598/aeee.v18i1.3511.

[4] BABA, A. O., G. LIU, X. CHEN. Classification and evaluation review of maximum power point tracking methods. *Sustainable Futures*. 2020, vol. 2. DOI: 10.1016/j.sftr.2020.100020.

[5] AHMED, J., Z. SALAM. An improved perturb and observe (P&O) maximum power point tracking (MPPT) algorithm for higher efficiency. *Applied Energy*. 2015, vol. 150, pp. 97-108. DOI: 10.1016/j.apenergy.2015.04.006.

[6] ELGENDY, M. A., B. ZAHAWI, D. J. ATKINSON. Operating characteristics of the P&O algorithm at high perturbation frequencies for standalone PV systems. *IEEE transactions on energy conversion*. 2014, vol. 30, no. 1, pp. 189-198. DOI: 10.1109/TEC.2014.2331391.

[7] DE BRITO, M. A. G., et al. Evaluation of the main MPPT techniques for photovoltaic applications. *IEEE transactions on industrial electronics*. 2012, vol. 60, no. 3, pp. 1156-1167. DOI: 10.1109/TIE.2012.2198036.

[8] SIVAKUMAR, P., A. A. KADER, Y. KALIAVARADHAN, M. ARUTCHELVI. Analysis and enhancement of PV efficiency with incremental conductance MPPT technique under non-linear loading conditions. *Renewable Energy*. 2015, vol. 81, pp. 543-550. DOI: 10.1016/j.renene.2015.03.062.

[9] XU, S.-Z., Y.-M. ZHONG. NSNPSO-INC: A Simplified Particle Swarm Optimization Algorithm for Photovoltaic MPPT Combining Natural Selection and Conductivity Incremental Approach. *IEEE Access*. 2024, vol. 12, pp. 137760-137774. DOI: 10.1109/ACCESS.2024.3463736.

[10] HMIDET, A., et al. Design of Efficient Off-Grid Solar Photovoltaic Water Pumping System Based on Improved Fractional Open Circuit Voltage MPPT Technique. *International Journal of Photoenergy*. 2021, vol. 2021, no. 1. DOI: 10.1155/2021/4925433.

[11] SHER, H. A., et al. A new sensorless hybrid MPPT algorithm based on fractional short-circuit current measurement and P&O MPPT. *IEEE Transactions on sustainable energy*. 2015, vol. 6, no. 4, pp. 1426-1434. DOI: 10.1109/TSTE.2015.2438781.

[12] GUL, S., S. M. MALIK, Y. SUN, F. ALSAIF. An Artificial Neural Network Based MPPT Control of Modified Flyback Converter for PV Systems in Active Buildings. *Energy Reports*. 2024, vol. 12, pp. 2865-2872. DOI: 10.1016/j.egyr.2024.08.082.

[13] EL HAMZAOUI, F. Z., T. ABDERRAHIME, B. D. TAOUFIQ. Comparison Between Perturb & Observe, Fuzzy Logic MPPT Technique, and The Artificial Neural Network Techniques at Different Temperature Conditions. *IFAC-PapersOnLine*. 2024, vol. 58, iss. 13, pp. 599-604. DOI: 10.1016/j.ifacol.2024.07.548.

[14] FATHI, M., J. A. PARIAN. Intelligent MPPT for photovoltaic panels using a novel fuzzy logic and artificial neural networks based on evolutionary algorithms. *Energy Reports*. 2021, vol. 7, pp. 1338-1348. DOI: 10.1016/j.egyr.2021.02.051.

[15] BISHT, R., A. SIKANDER. An improved method based on fuzzy logic with beta parameter for PV MPPT system. *Optik*. 2022, vol. 259. DOI: 10.1016/j.ijleo.2022.168939.

[16] ÁGUILA-LEÓN, J., et al. Optimizing photovoltaic systems: a meta-optimization approach with GWO-Enhanced PSO algorithm for improving MPPT controllers. *Renewable Energy*. 2024, vol. 230. DOI: 10.1016/j.renene.2024.120892.

[17] BORNI, A., et al. Optimized MPPT controllers using GA for grid connected photovoltaic systems, comparative study. *Energy Procedia*. 2017, vol. 119, pp. 278-296. DOI: 10.1016/j.egypro.2017.07.084.

[18] DINAKARAN, S. A., et al. Modelling and performance analysis of improved incremental conductance MPPT technique for water pumping system. *Measurement: Sensors*. 2023, vol. 30. DOI: 10.1016/j.measen.2023.100895.

[19] BOUARROUDJ, N., et al. A new tuning rule for stabilized integrator controller to enhance the indirect control of incremental conductance MPPT algorithm: Simulation and practical implementation. *Optik*. 2022, vol. 268. DOI: 10.1016/j.ijleo.2022.169728.

[20] ULLAH, K., et al. Fuzzy-based maximum power point tracking (MPPT) control system for photovoltaic power generation system. *Results in Engineering*. 2023, vol. 20. DOI: 10.1016/j.rineng.2023.101466.

[21] HAI, T., J. ZHOU, K. MURANAKA. An efficient fuzzy-logic based MPPT controller for grid-connected PV systems by farmland fertility optimization algorithm. *Optik*. 2022, vol. 267. DOI: 10.1016/j.ijleo.2022.169636.

[22] KAYISLI, K. Super twisting sliding mode-type 2 fuzzy MPPT control of solar PV system with parameter optimization under variable irradiance conditions. *Ain Shams Engineering Journal*. 2023, vol. 14, iss. 1. DOI: 10.1016/j.asej.2022.101950.

[23] YOUSSEF, A., M. EL TELBANY, A. ZEKRY. Reconfigurable generic FPGA implementation of fuzzy logic controller for MPPT of PV systems. *Renewable and Sustainable Energy Reviews*. 2018, vol. 82, pp. 1313-1319. DOI: 10.1016/j.rser.2017.09.093.

[24] AMMAR, H. H., et al. Metaheuristic Optimization of Fractional Order Incremental Conductance (FO-INC) Maximum Power Point Tracking (MPPT). *Complexity*. 2019, vol. 2019, iss. 1. DOI: 10.1155/2019/7687891.

[25] KABALCI, E., H. IRGAN, Y. KABALCI. Hybrid microgrid system design with renewable energy sources. *2018 IEEE 18th International Power Electronics and Motion Control Conference (PEMC), Budapest, Hungary*. 2018, pp. 387-392. DOI: 10.1109/EPEPEMC.2018.8521840.

[26] ISKANDAR, H. R., et al. Comparison model of buck-boost and zeta converter circuit using MPPT control incremental conductance algorithm. *2020 International Conference on Sustainable Energy Engineering and Application (ICSEEA), Tangerang, Indonesia*. 2020, pp. 185-190. DOI: 10.1109/ICSEEA50711.2020.9306121.

[27] ABOUOBAIDA, H., et al.Performance optimization of the INC-COND fuzzy MPPT based on a variable step for photovoltaic systems. *Optik*. 2023, vol. 278. DOI: 10.1016/j.ijleo.2023.170657.

[28] ATICI, K., N. ALTIN, İ. SEFA. Design of MPPT Method Based on Grey Wolf Optimization for Photovoltaic Systems. *In: 2019 3rd International Symposium on Innovative Approaches in Scientific Studies. Elazig: Turkey*. 2019. DOI:10.1109/ICPEA1.2019.8911159.

[29] VAIDEESWARAN, V., S. BHUVANESH, M. DEVASENA. Battery management systems for electric vehicles using lithium ion batteries. *2019 Innovations in Power and Advanced Computing Technologies (i-PACT), Vellore, India*. 2019, pp. 1-9. DOI: 10.1109/i-PACT44901.2019.8959965.

[30] KAYSAL, A., S. KÖROĞLU, Y. OĞUZ. Hierarchical energy management system with multiple operation modes for hybrid DC microgrid. *International Journal of Electrical Power & Energy Systems*. 2022, vol. 141. DOI: 10.1016/j.ijepes.2022.108149.

[31] KATCHE, M. L., et al. A comprehensive review of maximum power point tracking (mppt) techniques used in solar pv systems. *Energies*. 2023, vol. 16, no. 5. DOI: 10.3390/en16052206.

[32] OUNNAS, D., et al. Design and hardware implementation of modified incremental conductance algorithm for photovoltaic system. *Advances in Electrical and Electronic Engineering*. 2021, vol. 19, no. 2, pp. 100-111. DOI: 10.15598/aeee.v19i2.3881.

[33] SHANG, L., H. GUO, W. ZHU. An improved MPPT control strategy based on incremental conductance algorithm. *Protection and Control of Modern Power Systems*. 2020, vol. 5, no. 2, pp. 1-8. DOI: 10.1186/s41601-020-00161-z.

[34] REGAYA, C. B., et al. Real-time implementation of a novel MPPT control based on the improved PSO algorithm using an adaptive factor selection strategy for photovoltaic systems. *ISA Transactions*. 2024, vol. 146, pp. 496-510. DOI: 10.1016/j.isatra.2023.12.024.

[35] GAWANDE, M. K., et al. Modern approach for hybridization of PSO-INC MPPT methods for efficient solar power tracking. *2021 2nd Global Conference for Advancement in Technology (GCAT), Bangalore, India*. 2021, pp. 1-6. DOI: 10.1109/GCAT52182.2021.9587833.

[36] SANTOS, P., P. FONTE, R. LUIS. Improvement of DC Microgrid Voltage Regulation Based on Bidirectional Intelligent Charging Systems. *2018 15th International Conference on the European Energy Market (EEM), Lodz, Poland*. 2018, pp. 1-6. DOI: 10.1109/EEM.2018.8469991.